ELSEVIER

Polymer 42 (2001) 5189–5198

polymer

www.elsevier.nl/locate/polymer

Cure kinetics and ultimate properties of a tetrafunctional epoxy resin toughened by a perfluoro-ether oligomer

P. Musto[a,*], E. Martuscelli[a], G. Ragosta[a], L. Mascia[b]

[a]*Institute of Research and Technology of Plastic Materials, National Research Council of Italy, Via Toiano, 6 80072 Arco Felice, Naples, Italy*
[b]*Institute of Polymer Technology and Materials Engineering, Loughborough University, Loughborough, Leics LE 11 3TU, UK*

Received 10 July 2000; received in revised form 5 November 2000; accepted 27 November 2000

Abstract

A commercial grade of a tetrafunctional epoxy resin (TGDDM) has been modified by the addition of a perfluoro-ether oligomer to improve the toughness. The cure characteristics of a typical composition of this mixture have been investigated by in situ FT-NIR spectroscopy. It has been found that the presence of the fluoro-oligomer induces a two-fold reduction of the initial curing rate, which has been discussed in terms of the cure mechanism. For all the investigated compositions, the final conversion of the reactants did not change with respect to that of the unmodified resin. The phase structure of this system has been investigated by dynamic-mechanical analysis and by scanning electron microscopy. Both these techniques showed no evidence of a two-phase morphology. Finally, the fracture parameter G_c has been found to increase significantly for concentrations of the modifier exceeding 10 parts by weight.

Keywords: Epoxy resins; Fluoro-oligomer; Toughness

1. Introduction

Epoxy resins are an important class of thermosetting polymers, widely used in advanced technologies as, for instance, in the aerospace industry, in the electronic and communication fields and for storage and management of nuclear waste. However, these materials suffer two important limitations: they are intrinsically brittle and absorb considerable amounts of environmental moisture, which adversely affect most physico-mechanical properties. Both these drawbacks increase by enhancing the cross-link density of the network. In fact it has been shown that the increase in toughness achievable by rubber addition decreases strongly with enhancing the functionality of the epoxy monomer. The tendency to absorb water strongly depends on the polarity of the resin, that is, on the amount of hydroxyl groups formed on curing, which also increases with the monomer functionality. From the above considerations it follows that for a tetrafunctional epoxy resin such as the tetraglycidyl-4,4′-diaminodiphenyl-methane (TGDDM) the brittleness and the water sorption represent problems of considerable technological relevance. This is particularly so because of the very demanding applications in which this resin is employed.

The search for suitable toughening agents for these resins which could also be capable of reducing the moisture absorption [1], prompted several investigators to employ fluorinated polymers, in the form of reactive oligomers. For instance, Mascia et al. have used telechelic extended carboxyl-terminated perfluoro-oligomers to improve the toughness of bifunctional and tetrafunctional epoxy resins [1,2]. Curing this resin/fluoro-oligomer mixture with an anhydride hardener produced transparent materials, having heterophase morphology consisting of interpenetrating domains. By adjusting the curing conditions, it was also possible to obtain a fully phase separated system, consisting of fluoro-oligomer/epoxy domains dispersed in the epoxy matrix. A considerable increase in ductility (elongation at break) and toughness was achieved in this way, particularly in the case of particle dispersed systems. In the case of the tetrafunctional epoxy, the water sorption characteristics were also influenced by the presence of the fluoro-oligomer, with a decrease of the equilibrium water uptake and an increase of the ambient temperature diffusivity [1].

In the present contribution the above approach is extended to the case of a commercial TGDDM resin cured with methyl nadic anhydride. The mechanism and kinetics of curing of the modified resin is analysed in comparison to those of the unmodified system. FT-NIR spectroscopy has been employed to monitor in situ the time evolution of the reactive systems. Further information on the phase structure

* Corresponding author. Tel.: +39-081-8534169; fax: +39-081-8663378.
E-mail address: musto@irtemp.na.cnr.it (P. Musto).

0032-3861/01/$ - see front matter
PII: S0032-3861(00)00884-3

Table 1
Codes compositions and final conversion for the investigated mixtures (chemical formulae are given in the text)

Code	TGDDM (weight ratio)	NMA (weight ratio)	FO (weight ratio)	TGDDM (wt%)	MNA (wt%)	FO (wt%)	α_{max} (%)
F0	100	80	–	55.6	44.4	–	84.3
F5	100	80	5	54.1	43.2	2.7	82.4
F10	100	80	10	52.6	42.1	5.3	82.5
F15	100	80	15	51.3	41.0	7.7	81.6
F20	100	80	20	50.0	40.0	10.0	81.4
F30	100	80	30	47.6	38.1	14.3	79.6

of these multi-component materials has been obtained by dynamic-mechanical analysis, while fracture measurements at low strain rate have been performed to evaluate their toughness.

2. Experimental

2.1. Materials

The epoxy resin was a commercial grade of tetraglycidyl-4,4′-diaminodiphenyl-methane (TGDDM) supplied by Ciba–Geigy (Basel, Switzerland) and was cured by methylbicyclo-(2,2,1)-heptene-2,3 dicarboxylic acid anhydride (methyl nadic anhydride, MNA) from Fluka (Buchs, Switzerland). Benzyl dimethylaniline (BDMA) from Aldrich (Milwaukee, WI) was used as accelerator. The carboxyl-terminated perfluoro-ether oligomer (FO) was synthesised according to the methods described in Refs. [1,2].

The chemical formulas of the system components are reported herein:

(a) TGDDM — tetraglycidyl-4,4′-diaminodiphenyl-methane.

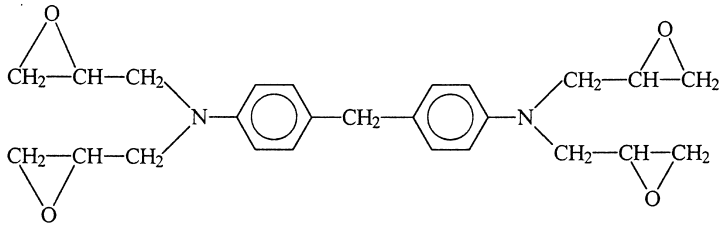

(b) MNA — methylbicyclo-(2,2,1)-heptene-2,3 dicarboxylic acid anhydride.

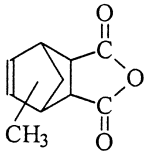

(c) FO — carboxy-terminated perfluoro-ether pre-polymer (1:1 mixture) ($z = 1.5$; p/q molar ratio $= 0.67$; $n = 10$).

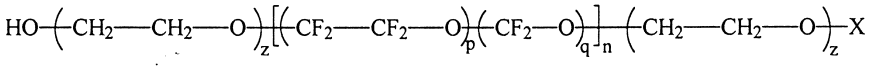

and

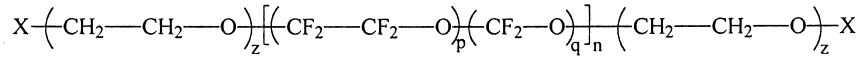

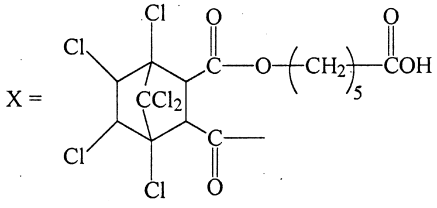

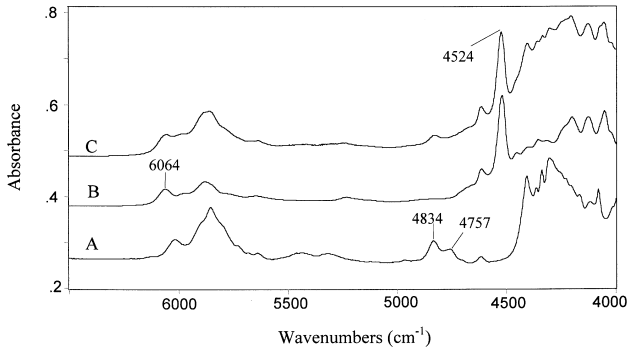

Fig. 1. FT-IR transmission spectra in the wavenumber range 6500–4000 cm^{-1} of MNA (trace A), uncured TGDDM (trace B) and uncured TGDDM/MNA mixture (trace C).

2.2. Preparation of a typical resin mixture

Eighty grams of MNA and the appropriate amount of FO (see Table 1) were dissolved into 100 g of TGDDM resin at 80°C under vigorous mechanical stirring. After complete dissolution, the mixture was cooled to room temperature and degassed under vacuum. 0.5 ml of BDMA (0.5 wt%) were added and the reactive mixture was poured in a glass mould, cured at 120°C for 4 h and post-cured at 170°C for 2 h. After this curing protocol, homogeneous and visually transparent samples were obtained in all cases.

The codes and compositions of the formulations examined are reported in Table 1. It is to be noted that the ratio of epoxy to anhydride components has been kept constant.

2.3. Characterization and evaluation techniques

Fourier transform infrared spectra in a near-IR range (8000–4000 cm^{-1}) were obtained in the transmission mode by a Perkin–Elmer System-2000 spectrometer. This instrument was equipped with a high temperature tungsten halogen NIR source, a multi-layer calcium fluoride beam-splitter and a deuterated triglycine sulphate (DTGS) detector. Thirty to three hundred spectra were co-added to improve the signal to noise ratio, at a resolution of 4 cm^{-1}. Isothermal kinetic measurements for the curing reactions were performed on samples 1.2 mm thick, in a Specac 80100 environmental chamber, directly mounted in the spectrometer and purged continuously with dry nitrogen. The chamber was controlled by an Eurotherm 071 temperature controller to an accuracy of ±0.5°C. The spectra collected on uncured samples, were obtained by sandwiching a drop of the reactive mixture between two glass windows.

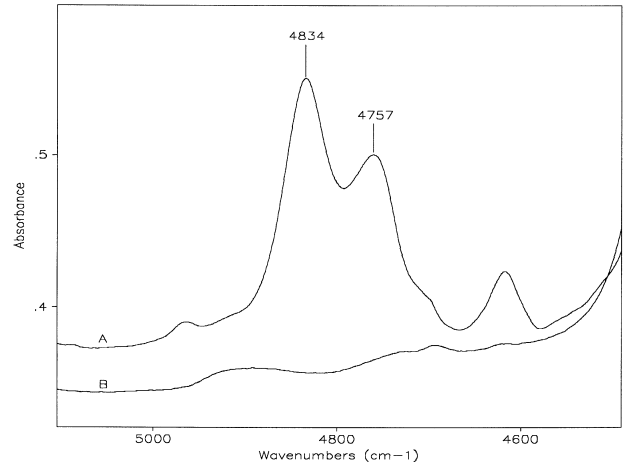

Fig. 2. FT-IR transmission spectra in the wavenumber range 5100–4500 cm^{-1} of MNA (trace A) and of the dimethyl ester obtained by methanolysis of MNA (trace B).

Dynamic-mechanical measurements were made at 1 Hz in the single-cantilever bending mode, using a dynamic mechanical thermal analyser (DMTA), Mod. MKIII from Polymer Laboratories, UK.

Three-point bending specimens $60.0 \times 6.0 \times 4.0\ mm^3$ were used to perform fracture tests at low strain rate. The measurements were carried out at room temperature on an Instron apparatus Mod. 4505 using a crosshead speed of 1 mm min^{-1}. Before testing, the samples were sharply notched with the aid of a circular saw and a razor blade. Fracture data were analysed according to the concepts of linear elastic fracture mechanics (LEFM) [3].

The critical strain energy release rate, G_c, was evaluated by the equation

$$G_c = \frac{U}{BW\phi} \tag{1}$$

where U is the fracture energy, B and W are, respectively, the thickness and the width of the specimen and ϕ is a calibration factor which essentially depends on the a/W ratio (a = initial crack length). Values of ϕ were taken from Plati and Williams [4].

3. Results and discussion

3.1. NIR spectroscopy of the reactive system

In Fig. 1 are reported the transmission FT-NIR spectra in the wave-number range 6500–4000 cm^{-1} for MNA (trace A), uncured TGDDM resin (trace B) and uncured F0 formulation (trace C). For a quantitative evaluation of the conversion of the various reactive groups, it is necessary to identify peaks characteristic of the epoxy group and of the anhydride functionality.

In the TGDDM spectrum two peaks characteristic of the oxirane ring can be identified at 6064 and at 4524 cm^{-1} [5]. The absorption at higher wavenumbers is due to the first overtone of the terminal CH_2 stretching mode, while the peak at lower wavenumbers has been attributed to a combination band of the second overtone of the epoxy ring stretch at 916 cm^{-1} with the fundamental C–H stretch at about 2725 cm^{-1} [6,7]. The 6064 cm^{-1} peak is highly

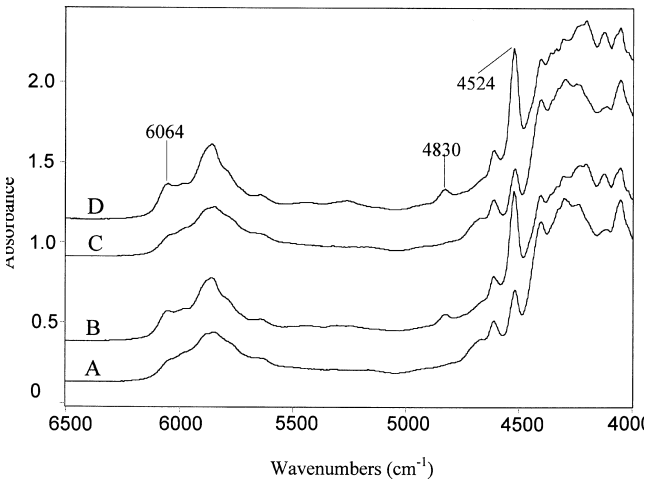

Fig. 3. FT-IR transmission spectra in the wavenumber range 6500–4000 cm^{-1} of the neat TGDDM/MNA resin (F0 composition) before and after the curing process (trace B and A, respectively), and the F20 composition before curing (trace D) and after curing (trace C).

overlapped with the complex profile at lower wavenumbers due to the C–H stretching overtones. This occurs to a larger extent in the TGDDM/MNA mixture (compare traces B and C) and, therefore, it cannot be directly used for quantitative analysis. Conversely, the peak at 4524 cm^{-1} is fully resolved, free from background interference and is suitable for concentration monitoring [8]. With respect to the anhydride group, a characteristic doublet is observed at 4834 and 4757 cm^{-1}, whose structure resembles that of the fundamental carbonyl stretching region, which displays two resolved components at 1858 and 1778 cm^{-1}, because of $\nu_{C=O,as}$ and $\nu_{C=O,s}$ modes., respectively. Thus, the NIR doublet is tentatively attributed to a combination of the above carbonyl fundamentals with a CH stretching vibration. The assignment of the 4834–4757 cm^{-1} doublet to an anhydride ring mode is confirmed by the spectra reported in Fig. 2 which compare the NIR spectra in the 5100–4600 cm^{-1} wavenumber range of MNA (trace A) and of its dimethyl ester, obtained by acid catalysed methanolysis (trace B). These show clearly that the peaks at 4834 and 4757 cm^{-1} completely disappear when the anhydride groups are esterified fully.

Further support to the above assignments is obtained by comparison of the NIR spectra of the F0 formulation before and after curing at 120°C for 4 h (traces B and A of Fig. 3, respectively). These show that the peaks characteristic of the epoxy groups at 6064 and 4524 cm^{-1} decrease considerably in intensity upon curing but remain still detectable, owing to incomplete conversion of the oxirane rings. The peak at 4830 cm^{-1} assigned to the anhydride rings, however, disappears completely in view of the two-fold stoichiometric excess of epoxy groups with respect to the anhydride groups. The characteristic peaks described above remain well detectable also in the presence, in the resin mixture, of the fluoro-oligomer, as shown in Fig. 3, traces D and C, which refer to the F20 formulation prior to and after curing.

3.2. Kinetic analysis of the curing process

Having recognised suitable analytical peaks, we proceeded to a kinetic analysis in order to investigate the effect of the fluoro-oligomer modifier on the mechanism and kinetics of the curing process, and to identify possible chemical interactions among the blend components. This analysis was performed on a typical blend composition containing 20 parts by weight of the fluoro-oligomer, and the results were eventually compared to those relative to the neat TGDDM/MNA mixture. The spectra collected at various reaction times in the two frequency ranges of interest are reported in Fig. 4A and B, while in Fig. 5 are shown the integrated absorbance values obtained from the spectra above, as a function of the reaction time. The data refer to the F0 formulation cured at 120°C.

From these absorbance values the relative conversion of the epoxy and anhydride groups can be evaluated as follows:

$$\alpha = \frac{C_0 - C_t}{C_0} = 1 - \frac{C_t}{C_0} \tag{3}$$

and, assuming the validity of the Beer–Lambert relation:

$$\alpha = 1 - \frac{A_t}{A_0} \tag{4}$$

where the symbols have the usual meaning and the subscripts 0 and t denote reaction times. No thickness correction was necessary, owing to the geometry of the sample holder that prevents thickness variation during the reaction.

All investigated compositions have a stoichiometric ratio, r, defined as mol anhydride groups/mole of epoxy groups, equal to 0.55. Owing to the epoxy excess over stoichiometry ($r < 1$), the concentration curves of epoxy and anhydride groups can be directly compared only if we consider the absolute conversion, $C_0 - C_t$, i.e. the moles of reactive group per unit mass consumed at time t. In terms of spectroscopic parameters, the absolute conversion is given by $C_0\alpha$, i.e. $C_0(1 - A_t/A_0)$.

The absolute conversion curves for the epoxy and anhydride groups relative to the F0 and F20 formulations, are reported, as a function of the reaction time, in Fig. 6. For both compositions the epoxy and anhydride conversion profiles are almost coincident in the early stages of the reaction, while diverging at later stages, where the curve relative to the epoxy groups predominates. The initial reaction rate is considerably higher in the case of the F0 formulation, while the final conversions for both anhydride and epoxy groups are about the same for the two investigated systems. A more quantitative analysis will be presented in the section on numerical modelling.

By plotting the data of Fig. 6 on an epoxy-anhydride conversion–conversion diagram, it is possible to establish

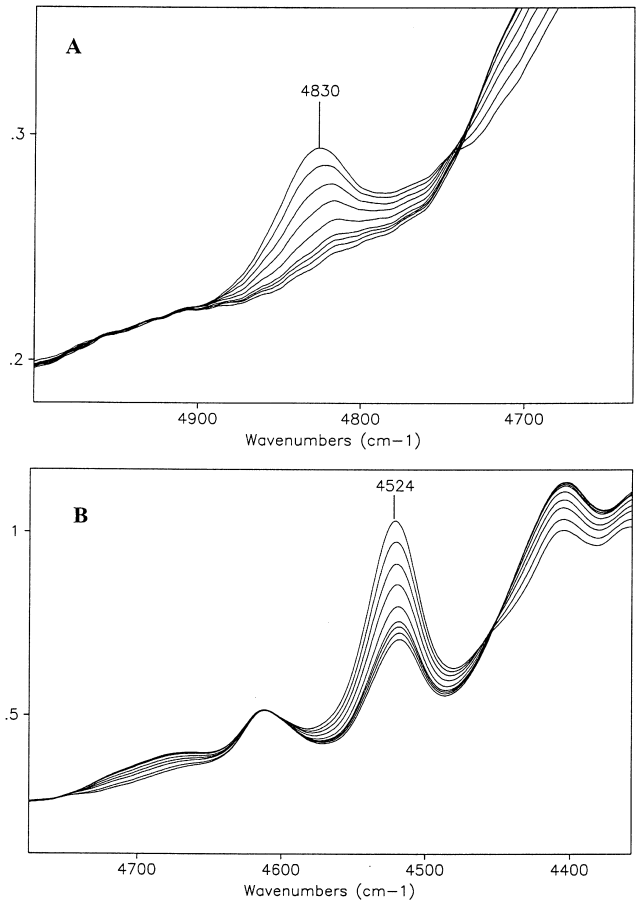

Fig. 4. *Real-time* spectroscopic monitoring of the curing reaction of the neat TGDDM/MNA resin: the two figures show the analytical wavenumber ranges: (A) 5000–4600 cm^{-1}; (B) 4800–4350 cm^{-1}. The spectra were collected at 120°C, at different reaction time.

the stoichiometry of the process and to detect changes of mechanism with conversion. A plot of this type is reported in Fig. 7 for both the F0 and F20 formulations. It is found that all data points can be accommodated on a single master curve. In particular, in the initial stages the data lie close to the iso-conversion line with slope equal to one, while at later stages, they bend upward, gradually deviating from the iso-conversion line. This indicates a mechanism whereby, in the presence of a sufficient concentration of hardener, a single epoxy group reacts with anhydride functionality, according to an alternating copolymerization mechanism which yields a cross-linked polyester network. The departure of the curves from the isoconversion line indicates the occurrence of side reactions (notably etherification) which consume epoxy groups only. The diagram of Fig. 7 demonstrates that, for both the unmodified resin and the FO containing formulation, these side reactions start to play a significant role towards the end of the curing process, when most of the anhydride groups have been consumed [9–11,15,16].

Thus, the presence of the fluoro-oligomer in the reactive

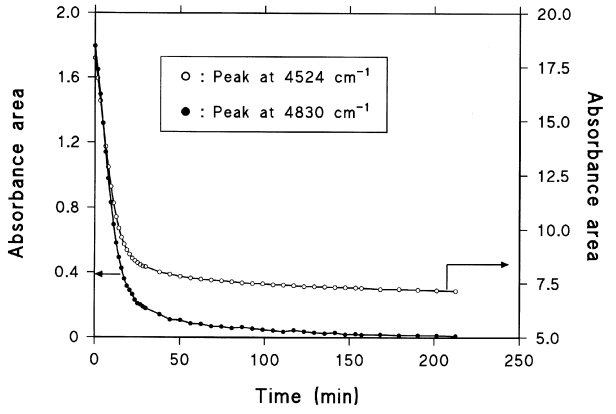

Fig. 5. Integrated absorbance as a function of the reaction time: (●) is obtained from the spectra reported in Fig. 4A; (○) is obtained from the spectra reported in Fig. 4B.

mixture has a strong retardation effect on the reaction kinetics, but it neither alters the overall stoichiometry of the curing process, nor promotes the occurrence of parasitic side reactions.

With respect to the mechanism of the curing process, an insight may be gained via numerical modelling of the kinetic behaviour [12–14].

The general reaction scheme for the amine catalysed cure of epoxides with anhydrides is reported in Scheme 1.

The unshared pair of electrons of the tertiary amine opens the anhydride ring with formation of a carboxyl anion. This step of the reaction is fairly fast. The reaction propagates by attack of the anion on the epoxy group to form an ester-alkoxide anion that can, in turn, react with anhydride to form an ester linkage and another carboxyl anion to propagate the reaction. The rate-determining step is believed to be the reaction between the anion and the epoxide. Therefore, in a

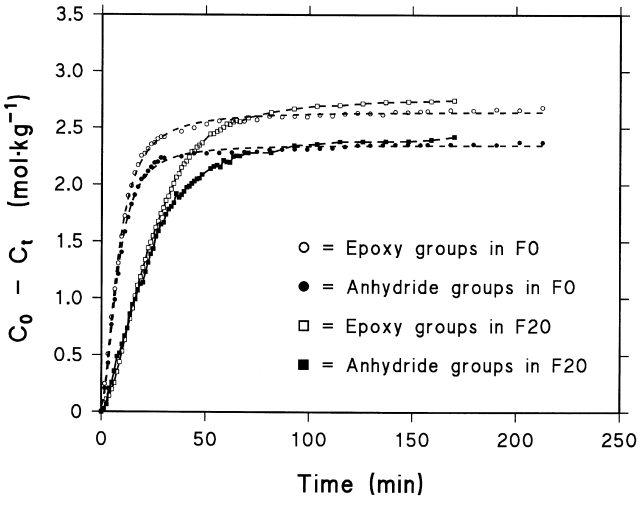

Fig. 6. Absolute conversion as a function of the reaction time for the epoxy and anhydride groups in the F0 and F20 formulations.

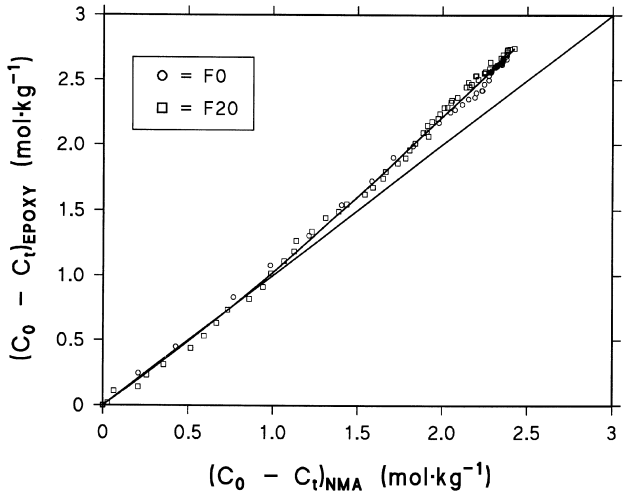

Fig. 7. Absolute conversion of epoxy groups vs absolute conversion of anhydride groups for the curing process at 120°C in the F0 and in F20 compositions (○ and □, respectively).

steady state regime, when the concentration of intermediate species is constant, the process is expected to be first order with respect to epoxide groups concentration [9–11,18].

In the light of the above considerations, the conversion versus time curve for the binary TGDDM/MNA mixture was simulated according to a nth order homogeneous kinetic model, of the form [9,11,16–18,31]:

$$\frac{d\alpha}{dt} = k(1-\alpha)^n \tag{5}$$

where n is an overall reaction order and k is an apparent reaction constant following an Arrhenius-type dependence with temperature. This simple model does not take into account that, as the conversion increases and the T_g of the material approaches the reaction temperature, the process becomes diffusion controlled. Thus the reaction rate decreases strongly, eventually reducing to zero before reaching full conversion of the reactants. This effect could be accounted for by substituting the term $(1-\alpha)$ in Eq. (5), with the term $(\alpha_{max}-\alpha)$, where α_{max} represents the final conversion reached at the investigated temperature [19]:

$$\frac{d\alpha}{dt} = k(\alpha_{max}-\alpha)^n \tag{6}$$

For the neat TGDDM/MNA mixture, the conversion rate of the epoxy groups, $d\alpha/dt$, evaluated numerically from the experimental α vs t data (Fig. 8, curve A) is reported, as a function of α, in Fig. 9, curve A. A non-linear, least-squares curve-fitting of the above data was performed by using Eq. (6), taking the k and n values as adjustable parameters. A satisfactory fit to the data points, represented by the continuous line was obtained, with a correlation coefficient, r^2, equal to 0.996. The k and n values obtained in this way were 0.094 min^{-1} and 1.00, respectively. Finally, the model

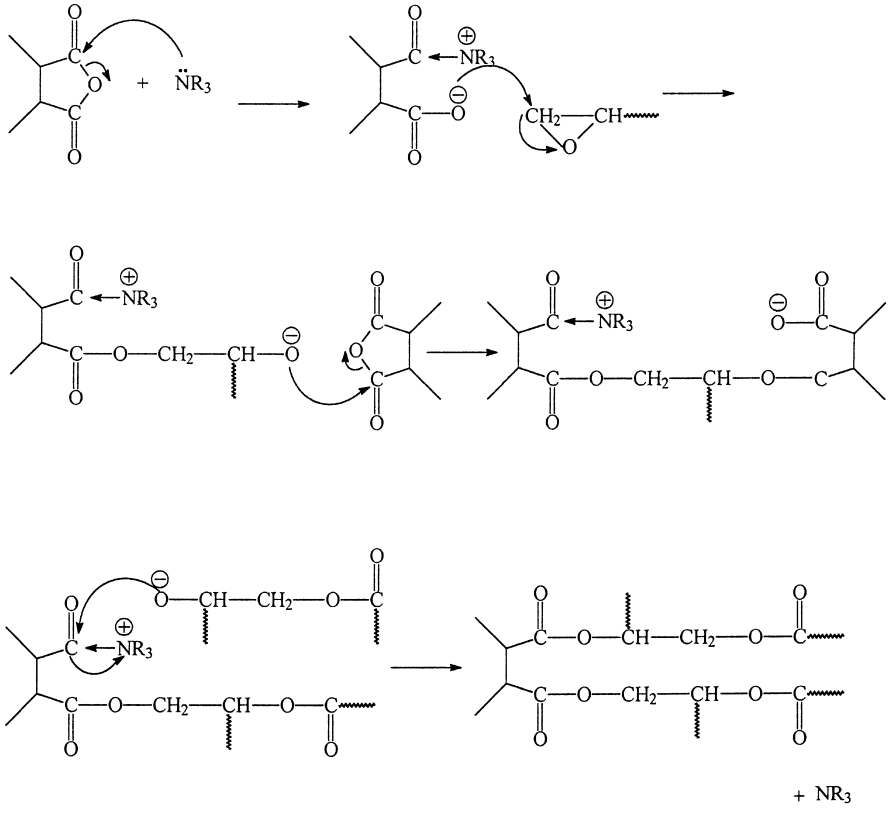

Scheme 1.

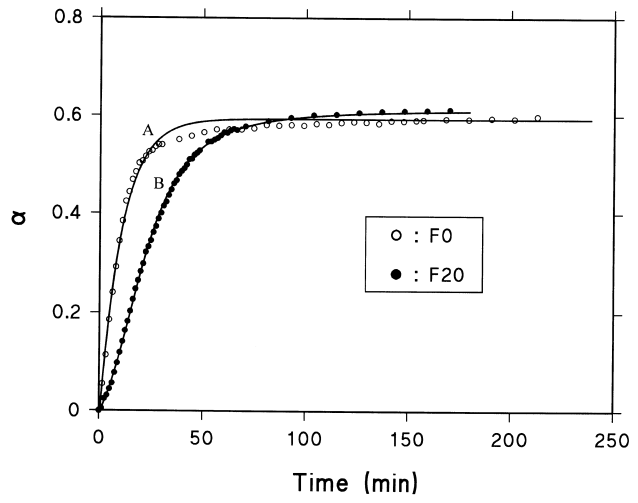

Fig. 8. Comparison among the experimental α vs t data (○, ●) and the conversion profiles simulated by the kinetic models (continuous lines). ○: F0 formulation; ●: F20 formulation.

equation was numerically integrated by the Runge–Kutta fourth order method to obtain the conversion profiles simulated by the model, to be compared with the experimental data. The simulated curve is reported in Fig. 8A as a continuous line. A reasonable agreement with the experiment is found, with a slight deviation toward the end of the process, when side reactions begin to play a significant role and the overall mechanism becomes more complex. Thus, the kinetic behaviour of the plain epoxy resin exhibits the first order dependence on epoxy groups concentration predicted by the reaction mechanism, which also implies a very rapid reaching of the steady state regime in the curing conditions used.

An analogous treatment was performed on the kinetic data relative to the F20 composition. The $d\alpha/dt$ vs the α curve obtained as above from the conversion profile of the

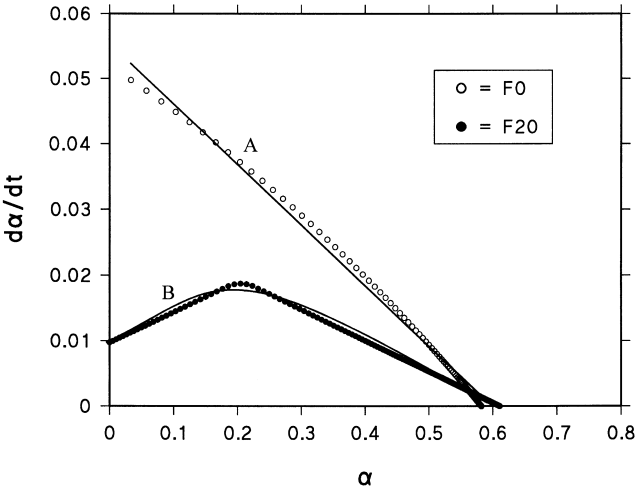

Fig. 9. Conversion rate, $d\alpha/dt$, as a function of relative conversion, α, for the epoxy groups in the F0 formulation (○) and in the F20 formulation (●). The continuous lines represents the curve obtained by best fitting of the experimental data with Eqs. (6) and (7).

epoxy groups (Fig. 8, curve B) is reported in Fig. 9, curve B. While for the binary TGDDM/MNA mixture the $d\alpha/dt$ vs time curve is linear, a pronounced maximum is observed for the F20 formulation, which results from the sigmoidal shape of the conversion profile relative to the latter mixture.

Clearly the model Eq. (6), being a monotonically decreasing function of α, is unable to fit the $d\alpha/dt$ vs α curve relative to the F20 composition, and a more complex model is needed. We attempted to use the single step autocatalytic model due to Kamal and co-workers [20,21], modified by taking into account the limiting conversion, which takes the form:

$$\frac{d\alpha}{dt} = (k_1 + k_2\alpha^m)(\alpha_{max} - \alpha)^n \quad (7)$$

This equation has been successfully used to describe the kinetic behaviour of complex thermosetting systems as amine cured epoxy resins [23], anhydride cured epoxies [38,39], unsaturated polyester resins [24] and thermosetting bismaleimides [25]. It consists of two terms, whereby k_1 represents the kinetic constant of the unperturbed reaction mechanism analogous to that of Eq. (6), and the term $k_2\alpha^m$ accounts for the presence of a co-catalyst and/or reactant that may influence the overall reaction mechanism. In the case of amine cured epoxies, this term accounts for the autocatalytic nature of the process [22].

The agreement between the conversion profile predicted by Eq. (7) and the experimental data is very satisfactory (see Fig. 8, curve B). The model is able to simulate the kinetic behaviour of the system over the whole conversion range. The m and n values are 0.92 and 1.40, respectively, while the k_1 and k_2 values are equal to 0.017 and 0.180 min^{-1}.

Finally, it is noted that the initial reaction rate, evaluated from the slope of the linear regime of the α–t curves, is found to be 0.035 min^{-1} for the plain epoxy resin and 0.017 min^{-1} for the F20 composition. This considerable retardation effect, brought about by a relatively small amount of fluoro-oligomer (about 10 wt% of the total content) could be due to a viscosity effect. The fluoro-oligomer dissolved in the TGDDM/MNA mixture increases strongly the viscosity of the reactive mixture and reduces the molecular mobility of the reactants.

Another possibility to account for the above effect is the formation of a quaternary ammonium salt between the carboxyl end-groups of the fluoro-oligomer and the tertiary amine catalyst. This will reduce the amount of active catalytic groups thereby lowering the overall reaction rate.

The presence of the fluoro-oligomer also induces a modification of the curing mechanism, as indicated by the fact that a more complex model equation is necessary to simulate the kinetic behaviour of the modified system. This effect is due to the simultaneous presence, in the F20 mixture, of more functional groups than in the F0 mixture. In particular, the carboxyl end-groups of the fluoro-oligomer may directly participate to the curing process and/or may influence in a complex manner the catalytic activity of the initiator. The

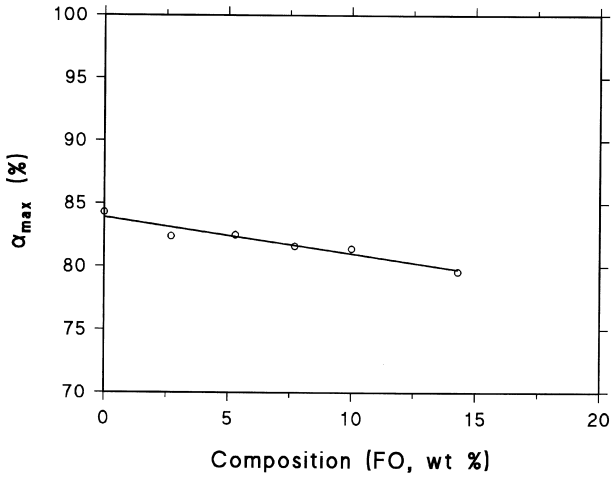

Fig. 10. Final conversion, α_f, of epoxy groups as a function of the fluoro-oligomer content in the system.

fluoro-oligomer molecules terminated at both ends with carboxylic functionalities, reacting with epoxy groups, can be incorporated within the thermosetting network. This chemical interaction hinders the phase separation process of the fluoro-oligomer during curing, enhancing phase homogeneity, as suggested by the visual transparency of the material.

The FT-NIR spectrum was collected for all the investigated compositions in order to determine the maximum conversion, α_{max}, of anhydride and epoxy groups after the curing and post-curing protocol. No residual anhydride groups were detected for any samples, while the epoxy conversion was always incomplete. In Fig. 10 are reported the α_{max} values relative to the epoxy groups as a function of the fluoro-oligomer content; it is found that α_{max} is scarcely affected by the amount of modifier present, decreasing from 84 to 80% in going from the plain epoxy resin to the F30 composition.

3.3. Dynamic-mechanical analysis and fracture properties

Dynamic mechanical spectra in terms of tan δ are reported in Fig. 11 for the neat TGDDM/MNA resin (solid line) and for the F20 composition (dotted line) after the curing and post-curing process. Both the materials exhibit a primary tan δ peak, corresponding to the T_g, at the same temperature (197°C). Similar results are obtained for all the investigated compositions. What is relevant in the above analysis, is the absence, in the tan δ spectrum of all the investigated blends, of any relaxation peak in the temperature range were the glass transition of the fluoro-oligomer is expected to occur (between −50 and −40°C).

This indicates that no phase separation of the modifier takes place during the curing and post-curing processes, at least to the scale of the dynamic-mechanical analysis, i.e. to the size of the segments responsible for the primary relaxation mechanisms.

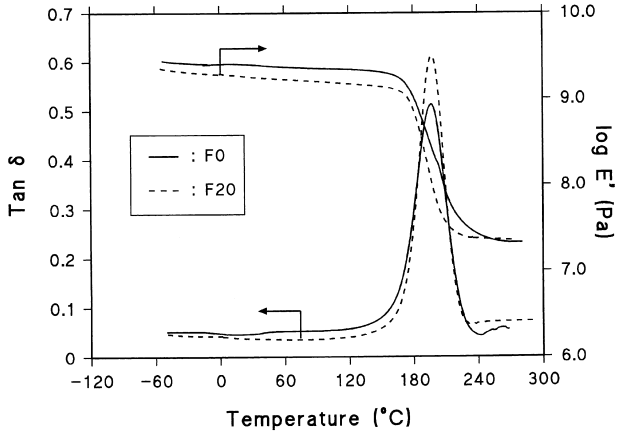

Fig. 11. Dynamic-mechanical spectra in terms of tan δ and storage modulus, E', for TGDDM/MNA resin (solid line) and F20 composition (dotted line) after the curing and post-curing process.

This result has been confirmed by scanning electron microscopy (SEM) analysis of the fracture surfaces of the blends (not reported), which do not provide any evidence of a second phase within the epoxy matrix, even at very high magnification (10,000×).

On the cured and post-cured materials, a fracture analysis was performed at room temperature and at low deformation rate (1.0 mm min^{-1}), to test the capability of the fluoro-oligomer to effectively toughen the epoxy matrix.

The critical strain energy release rate, G_c, evaluated according to Eq. (1), is reported in Fig. 12 as a function of the amount of fluoro-oligomer in the blend. It is noted that, up to about 10 parts by weight of modifier, G_c remains essentially constant. However, an abrupt increase of this parameter occurs at higher contents of the modifier. In the same diagram are also reported the flexural elastic moduli of the investigated blends. A linear decrease in modulus with increasing FO concentration is observed over the range examined, with a less than 20% reduction relative to the control resin for a FO content of 14.7%.

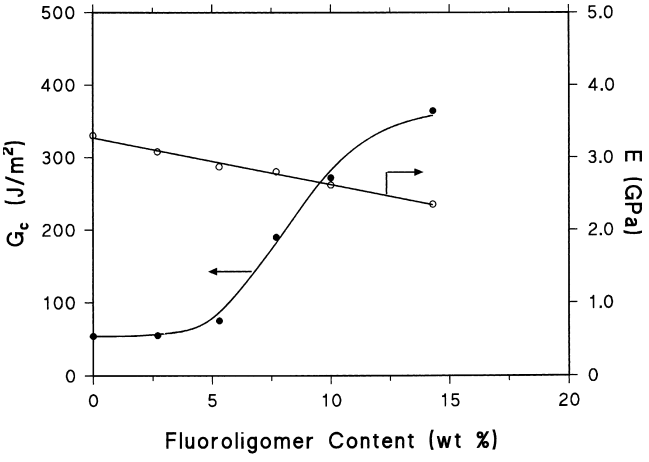

Fig. 12. Critical strain energy release rate, G_c, and flexural elastic modulus, E, as a function of blend composition.

For a tetrafunctional epoxy resin the above increase in toughness represents a significant result, since these systems are extremely difficult to toughen. In fact, for densely cross-linked networks, the conventional approach consisting in the addition of low molecular weight reactive rubbers was unsuccessful. This is because the capability of the matrix to be plastically deformed decreases strongly by increasing the cross-linking density. Thus, the rubber particles are no longer able to induce energy dissipation mechanisms such as localised shear yielding of the matrix initiated by the rubber particles, and/or cavitation of the rubbery domains [26–28].

In these cases an alternative approach has been recently devised, based on the incorporation of tough, ductile and thermally stable engineering thermoplastics [26,29–35]. The thermoplastic component can be simply mixed with the matrix, giving rise to a completely phase separated system after curing or can be incorporated within the thermosetting network by means of suitable reactive blending processes, thus rendering the whole network more deformable under loading. In the latter case, to take full advantage of the modifier, the phase separation of the minor component is to be avoided, so as to obtain a molecularly homogeneous system. The approach of incorporating flexible segments within the thermosetting network can be adopted also with functional liquid rubbers as second components. Obviously, in this case, the need to avoid phase separation becomes even more stringent.

For thermoplastic modified systems, interesting results were found by some of us using both the approaches outlined above. Considerable improvements of toughness were achieved with phase separated systems consisting of TGDDM/polyetherimide blends [34,35] and bismaleimide/polyetherimide blends [34,36] For molecularly homogeneous systems, equally interesting results were obtained with a tri-functional epoxy/polycarbonate system [31,32,35] and with a blend consisting of a thermosetting bismaleimide modified by an imide-terminated butadiene-acrylonitrile copolymer [25,36,37].

According to dynamic-mechanical and SEM analyses, the system reported in the present investigation seems to fall in the category of single phase networks. Therefore, the observed toughening enhancement could be due to the enhanced capability of the whole network to be plastically deformed under loading for the presence of the flexible fluoro-oligomer chains into the network. This effect, further confirmed by the decrease of the elastic modulus with increasing FO content, becomes significant, in terms of toughness, when a critical amount of flexible chains are present in the system, thereby increasing with the content of modifier (see Fig. 12). However, the possibility of phase separated domains whose size lies beyond the detectability limits of dynamic-mechanical analysis and SEM microscopy cannot be ruled out. Further investigations based on Small Angle X-Ray Scattering (SAXS) measurements are currently underway to elucidate this point.

4. Conclusions

A reactive fluoro-oligomer was used as toughening agent for a highly cross-linked epoxy resin. Blends with various amounts of the modifier were prepared and investigated. A kinetic analysis of the curing process showed that the presence of the fluoro-oligomer induces a significant decrease of the reaction rate, which has been tentatively ascribed to a viscosity enhancement and/or to interactions of the modifier with the tertiary amine catalyst. Conversely, for all the investigated compositions, the final conversion of the reactants was found to remain essentially unaffected with respect to the plain epoxy resin. The curing mechanism has been also considered. It was found that, to correctly simulate the kinetic behaviour of a blend system, a more complex model is necessary than that used for the neat resin. This effect has been attributed to the active participation of the fluoro-oligomer to the curing process, through its reactive end-groups.

Dynamic-mechanical measurements and SEM analysis showed no evidence of phase separation of the minor component during the curing and post-curing processes.

The fracture results demonstrated a consistent enhancement of the toughness parameter G_c when the modifier reaches a critical concentration in the system ($\geq$10 parts by weight). This improvement was attributed to the chemical incorporation of flexible fluoro-oligomer segments into the epoxy network, which enhances its ability to be plastically deformed during the fracture process.

References

[1] Martuscelli E, Musto P, Ragosta G, Riva F, Mascia L. J Mater Sci 2000;35:3719.
[2] Mascia L, Zitouni F, Tonelli C. Polym Engng Sci 1995;35:1069.
[3] Williams JG. Fracture mechanics of polymers. Chichester: Ellis Horwood, 1989.
[4] Plati E, Williams JG. Polym Engng Sci 1975;15:470.
[5] Musto P, Martuscelli E, Ragosta G, Russo P. High Perform Polym 2000;12:155.
[6] Xu L, Schlup JR. Appl Spectrosc 1996;50:109.
[7] George GA, Cole-Clarke P, St. John N, Friend G. J Appl Polym Sci 1991;42:643.
[8] Mijovic J, Andjelic S, Kenny JM. Polym Adv Technol 1996;7:1.
[9] Ellis B. Chemistry and technology of epoxy resins. London: Blackie, 1993.
[10] Matêjka L, Lövy J, Pokornú S, Bouchal K, Dušek K. J Polym Sci A: Polym Chem 1983;21:2873.
[11] Antoon MK, Koenig JL. J Polym Sci A: Polym Chem 1981;19:549.
[12] Bokare UM, Ghandi KS. J Polym Sci A: Polym Chem 1980;18:857.
[13] Morgan RJ, Mones ET. J Appl Polym Sci 1987;33:999.
[14] Tsou AH, Peppas NH. J Polym Sci B: Polym Phys 1988;26:2043.
[15] Stevens GC. J Appl Polym Sci 1981;26:4259.
[16] Corcuera MA, Mondragon I, Riccardi CC, Williams RJJ. J Appl Polym Sci 1997;64:157.
[17] Barton JM. Adv Polym Sci 1985;72:111.
[18] Woo EM, Seferis JC. J Appl Polym Sci 1990;40:1237.
[19] Martuscelli E, Musto P, Ragosta G, Russo P, Villano P. Submitted for publication.
[20] Kamal MR, Sourour S. Polym Engng Sci 1973;13:59.

[21] Kamal MR, Sourour S, Ryan MR. SPIE Tech Pap 1973;19:187.
[22] Keenan MR. J Appl Polym Sci 1987;33:1725.
[23] Fu JH, Schulp JR. J Appl Polym Sci 1993;49:219.
[24] Dell'Erba R, Martuscelli E, Musto P, Ragosta G. Polym Networks Blends 1997;7(1):1.
[25] Martuscelli E, Musto P. In: Martuscelli E, Musto P, Ragosta G, editors. Advanced routes for polymer toughening. Amsterdam: Elsevier, 1995 (chap. 3; p. 121).
[26] Martuscelli E, Musto P. In: Martuscelli E, Musto P, Ragosta G, editors. Advanced routes for polymer toughening. Amsterdam: Elsevier, 1995 (chap. 1; p. 11).
[27] Kinloch AJ, Shaw SJ, Hunston DL. Polymer 1983;24:1355.
[28] Kinloch AJ, Young RJ. Fracture of polymers. London: Applied Science Publishers, 1983 (421 p).
[29] Bucknall CB, Partridge IK. Polymer 1983;24:339.
[30] Bucknall CB, Partridge IK. Polym Engng Sci 1986;26:54.
[31] Abbate M, Martuscelli E, Musto P, Ragosta G, Scarinzi G. J Polym Sci B: Polym Phys 1994;32:395.
[32] Di Liello V, Martuscelli E, Musto P, Ragosta G, Scarinzi G. J Polym Sci B: Polym Phys 1994;32:409.
[33] Martuscelli E, Musto P, Ragosta G, Scarinzi G. Die Ang Makromol Chem 1993;204:153.
[34] Martuscelli E, Musto P, Ragosta G, Scarinzi G. Die Ang Makromol Chem 1993;213:93.
[35] Martuscelli E, Musto P, Ragosta G, Scarinzi G. Die Ang Makromol Chem 1994;217:159.
[36] Martuscelli E, Musto P, Ragosta G, Scarinzi G. Die Ang Makromol Chem 1997;246:23.
[37] Abbate M, Martuscelli E, Musto P, Ragosta G, Leonardi M. J Appl Polym Sci 1996;62:2107.
[38] Monserrat S, Malek J. Thermochim Acta 1993;228:47.
[39] Vyazovkin S, Sbirazzuoli N. Macromol Chem Phys 1999;200:2294.